Galaxy Zoo Builder: Morphological Dependence of Spiral Galaxy pitch angle

Timothy Lingard[1]⋆, Karen L. Masters[2], Coleman Krawczyk[1], Chris Lintott[3],
Sandor Kruk[4], Brooke Simmons[5], William Keel[6], Robert C. Nichol,[1]
Elisabeth Baeten[7]

[1] *Institute of Cosmology and Gravitation, University of Portsmouth, Dennis Sciama Building, Burnaby Road,*
Portsmouth, PO1 3FX, UK
[2] *Haverford College, 370 Lancaster Ave., Haverford, PA 19041, USA*
[3] *Oxford Astrophysics, Denys Wilkinson Building, Keble Road, Oxford, OX1 3RH, UK*
[4] *European Space Agency, ESTEC, Keplerlaan 1, NL-2201 AZ, Noordwijk, The Netherlands*
[5] *Physics Department, Lancaster University, Lancaster, LA1 4YB, UK*
[6] *Department of Physics & Astronomy, University of Alabama, Tuscaloosa, AL 35457-0324*
[7] *Independent Zooniverse Volunteer*

ABSTRACT
Spiral structure is endemic in the Universe, and the pitch angle of arms in spiral galaxies is an important observable in efforts to discriminate between different mechanisms of spiral arm evolution. In this paper we present a hierarchical Bayesian approach to galaxy pitch angle determination, using spiral arm data obtained through the *Galaxy Builder* citizen science project (Lingard et al. 2020). This approach better deals with the large variations in pitch angle between arms in a galaxy than existing methods, and obtains full posterior distributions on parameters. We utilise fit pitch angles to examine the links to morphology reported in other work, finding no link in our data, and find consistency in our results with a simple model of spiral winding, proposed by Pringle & Dobbs (2019), which assumes the uniformity of the cotangent of pitch angle between some unknown upper and lower limits.

Key words: galaxies: evolution – galaxies: spiral – galaxies: photometry

1 INTRODUCTION

Spiral structure is present in a majority of massive galaxies (Buta 1989, Lintott et al. 2008) yet the formation mechanisms through which spiral structure originates are still hotly debated. Spirals are as diverse as the theories proposed to govern their evolution; from the quintessential pair of well-defined arcs of the grand design spiral, to the fragmented arm segments of the flocculent spiral, to the disjointed multi-armed spiral. These variations on structure account for 18%, 50% and 32% of the population respectively (Elmegreen et al. 2011, Buta et al. 2015, examples of each type are shown in Figure 1). The Hubble classification scheme (Hubble 1926), and its revisions and expansions (Sandage 1961, de Vaucouleurs et al. 1991) contain detailed variations of different types of spiral galaxy, divided by the presence of a bar and ordered by how obvious spiral arm patterns are,

how tightly they are wound and the prominence of a central bulge.

A majority of the population of young stars in a galaxy are located in its spiral arms (Elmegreen 2011), and it is possible that their passage triggers star formation (Cedrés et al. 2013), though their main role may instead be to sweep up material, promoting the growth of Giant Molecular Clouds. (Dobbs 2014). This rearrangement of disc gas can lead to the formation of disc-like bulges (commonly called "pseudobulges"; e.g. Kormendy & Kennicutt 2004). Studies of spiral morphology have found interesting correlations between spiral morphology and other galactic properties, such as a correlation between spiral tightness and central mass concentration (Yu & Ho 2019, though Hart et al. 2017 found no such relation) and tightness and rotation curve shape (Seigar et al. 2005, with rising rotation curves creating more open spiral structure). These predictions and observations provide compelling reasons for investigating their
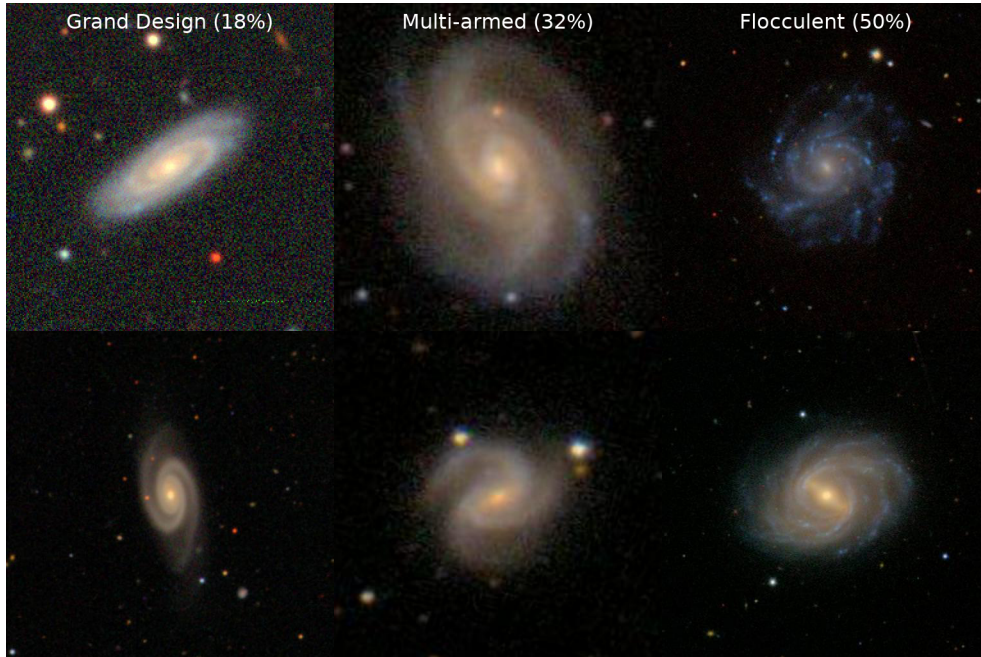
⋆ E-mail: tklingard@gmail.com

Figure 1. Examples of the different types of spiral galaxy present in the sky. The left column shows grand design spirals, the middle shows many-armed spirals and the right shows flocculent spirals. Images were taken with the Sloan Digital Sky Survey Telescope.

underlying rules and dynamics, as doing so is essential for understanding the secular evolution of disc galaxies.

Our current understanding of the mechanisms which drive spiral growth and evolution suggests that each of the different forms of spiral galaxy may be triggered primarily by different processes. Grand Design spirals are thought to have undergone a tidal interaction, be driven by a bar (as seen in gas simulations, Sanders & Huntley 1976, Rodriguez-Fernandez & Combes 2008, and suggested for stars by Manifold theory, Romero-Gómez et al. 2006, Athanassoula et al. 2009a, Athanassoula et al. 2009b), or be obeying (quasi-stationary) density wave theory (QSDW theory), in which spiral arms are slowly evolving, ever-present structures in the disc (Lin & Shu 1964). Flocculent spirals are thought to be formed through swing amplification (shearing of small gravitational instabilities in the disc), and be transient and recurrent in nature (Julian & Toomre 1966).

One of the fundamental assumptions of early work on spiral formation mechanisms (primarily QSDW) was that the disc of a galaxy, if unstable to spiral perturbations, would create a stable, static wave which would exist unchanging for many rotational periods (Lin & Shu 1964). The motivation for static waves with small numbers of arms (with a preference for $m = 2$) was primarily observational; most disc galaxies show spiral structure with low spiral arm numbers, suggesting that spirals exist for a long time or are continually rebuilt.

Many simulations demonstrate that spirals do not maintain a constant pitch angle, and instead wind-up over time due to the differential rotation of the disc (Baba et al. 2013). Recent research suggests that spirals arms are transient in nature, and continually dissipate and re-form (Dobbs & Baba 2014). These spirals can be maintained through the same mechanisms that drive QSDW spirals (i.e. WASER, Mark 1976, swing amplification, Goldreich & Lynden-Bell

1965), but do not require the idealistic disc conditions required for the formation and maintenance of a stationary wave. The pitch angles of these transient spiral arms will decrease due to the differential rotation of the disk, with the density of the arm peaking at some critical pitch angle, before dissipating to be reformed.

In this dynamic picture of spiral arms, pitch angle monotonically decreases from a spiral arm's formation to its dissipation. Pringle & Dobbs (2019) propose a simple test of spiral arm winding, assuming the cotangent of the pitch angle of a spiral arm evolves linearly with time. They found that the distribution of pitch angles of their sample of 86 galaxies was consistent with this prediction, evidence against QSDW theory in favour of the dynamic spirals produced in many simulations.

We aim to test this idea of spiral winding using data from the *Galaxy Builder* citizen science project for the spiral galaxies present in Lingard et al. (2020). We make use of Bayesian hierarchical modelling to measure galaxy pitch angle from the spiral arm clusters produced by *Galaxy Builder*. This methodology allows us to quantify the differences in pitch angles between arms in a single galaxy, as well as investigate the distribution of pitch angles in the galaxy population and investigate relationships between pitch angle and galaxy morphology.

Using Galaxy Zoo 2 data (Willett et al. 2013) allows the separation of galaxies by the presence and strength of a stellar bar; simulations of gas in barred galaxies often demonstrate that bars can drive long-term spiral evolution (Rodriguez-Fernandez & Combes 2008), or boost transient spiral structure (Grand et al. 2012). Manifold theory is one attempt to determine the orbits of stars in bar-driven spiral arms: it proposes that stars in the vicinity of the unstable Lagrangian points at either end of the bar tend to escape along predictable orbits, governed by invariant man-

ifolds. One of the primary factors influencing the shape of this invariant manifold is the relative strength of the non-axisymmetric forcing caused by the bar, with stronger bars resulting in spirals with larger pitch angles.

Many other systems correlate with spiral morphology, including potential ties to bulge fraction (Yoshizawa & Wakamatsu 1975, Savchenko & Reshetnikov 2013, Masters et al. 2019) and black hole mass (Seigar et al. 2008, Davis et al. 2017, Al-Baidhany et al. 2019). Stronger bulges and more massive central black holes have both correlated with more tightly wound spiral arms.

Section 3.3 investigates spiral arm winding using the test derived by Pringle & Dobbs (2019) (uniformity of galaxy pitch angle in cot ϕ). Section 3.2 examines the correlation between pitch angle and bulge size implied by the Hubble sequence, and pitch angle and bar strength implied by Manifold theory.

Where necessary, we make use of $H_0 = 70 \text{ km s}^{-1} \text{ Mpc}^{-1}$.

2 METHOD

2.1 Measuring galaxy pitch angle

Many methodologies have been proposed and implemented to measure spiral arm properties, including visual inspection (Herrera-Endoqui et al. 2015), Fourier analysis (i.e. 2DFFT, Davis et al. 2012), texture analysis (i.e. SpArcFiRe, Davis & Hayes 2014), and combinations of automated methods and human classifiers (Hart et al. 2017, Hewitt & Treuthardt 2020). One potentially underused method of obtaining measurements of spirals is through photometric fitting of spiral structure, as possible using tools such as GALFIT (Peng et al. 2010) and *Galaxy Builder* (Lingard et al. 2020). These methods attempt to separate light from an image of a galaxy into distinct subcomponents, such as a galaxy disc, bulge, bar and spiral arms, generally finding the optimum solution using computational optimization. This optimization process, however, is often not robust for complex, many-component models and requires significant supervision to converge to a physically meaningful result (Gao & Ho 2017). Lingard et al. (2020) propose a solution to this problem through the use of citizen science to provide priors on parameters used in computational fitting.

A common assumption when measuring galaxy pitch angle is that observed spiral arms have a constant pitch angle. Spirals of this kind are known as logarithmic spirals and are described by

$$r = A \, e^{\theta \tan \phi}, \tag{1}$$

where ϕ is the arm's pitch angle. One method used to obtain a pitch angle of a galaxy is to fit logarithmic spirals to individually identified arm segments and take the weighted mean of their pitch angles (which often vary by upwards of $10°$, Davis & Hayes 2014). Weighting is determined by the length of the arc segment, with longer being assigned higher weights, i.e. for a galaxy where we have identified N arm segments, each with length L_i and pitch angle ϕ_i

$$\phi_{\text{gal}} = \left(\sum_{i=1}^{N} L_i \right)^{-1} \sum_{i=1}^{N} L_i \phi_i. \tag{2}$$

The most commonly used measurement of uncertainty of length-weighted pitch angles is the unweighted sample variance between the arm segments identified.

A notable drawback of length-weighted pitch angle is sensitivity to the number and quality of the spiral arm segments identified; Hart et al. (2017) found that only 15% of the arm segments identified using SpArcFiRe were identified as "good" matches to real spiral arms by citizen science classifiers.

Fourier analysis in one- and two-dimensions (as performed by Díaz-García et al. 2019, Davis et al. 2012, Mutlu-Pakdil et al. 2018) is another widely used method of computationally obtaining galaxy pitch angles. Two-dimensional Fourier methods generally decompose a deprojected image of a galaxy into a superposition of logarithmic spirals between inner and outer annuli (Davis et al. 2012) and reports the pitch angle with the highest amplitude as the galaxy's pitch angle. Hewitt & Treuthardt (2020) combined Fourier analysis of spiral galaxies with visual tracing of spiral arms, to great effect. It is uncertain how the variation between pitch angles of individual arms impacts this measurement.

2.2 The Galaxy Sample

The galaxies analysed in this paper are those for which photometric models were obtained in Lingard et al. (2020). These are a subset of the *stellar mass-complete sample* in Hart et al. (2017), a sample of low-redshift face-on spiral galaxies selected using data from the NASA-Sloan Atlas (Blanton et al. 2011) and Galaxy Zoo 2 (Willett et al. 2013).

Some galaxies in Lingard et al. (2020) were shown to volunteers a second time in a repeat *validation subset* in order to create a second aggregate model used to test internal consistency. We combine the classifications of galaxies in this *validation subset* with the original classifications. Clustering of drawn spiral arms and cleaning of points was then performed as detailed in Lingard et al. (2020). We remove any galaxies for which no spiral arms were identified, resulting in a hierarchical data structure of 139 galaxies, 261 spiral arms and 239,947 points.

As we wish to utilize the logarithmic spiral's desirable properties of a constant pitch angle and a small number of free parameters, we make use of it here without an explicit comparison to other models; a simple visual inspection of the fitted logarithmic spirals suggests that it is an appropriate model. A comparison of a logarithmic spiral profile to other spiral forms (i.e. Archimedian or polynomial) is another important piece of work, outside of the scope of this research, as it has been reported that galaxy arms do not have constant pitch angles (Kennicutt 1981; Ringermacher & Mead 2009).

Spiral arm points are deprojected to a face-on orientation using the disk inclination and position angle obtained through photometric model fitting performed in Lingard et al. (2020). Arms are individually corrected to all have the same chirality (a pitch angle greater than or equal to zero) using the logarithmic spiral fit in Lingard et al. (2020).

2.3 Bayesian modelling of spiral arms in *Galaxy Builder*

In this Section, we lay out our bayesian hierarchical model for galaxy pitch angle. We fit directly to clustered, cleaned points from polylines drawn in *Galaxy Builder*, deprojected and unwrapped to polar coordinates. We fit a logarithmic spiral to each clustered arm, with the pitch angles of multiple arms in a single galaxy being drawn from a single parent distribution.

We assume that a galaxy has some value for pitch angle, ϕ_{gal}, and that the pitch angles of spiral arms in that galaxy, ϕ_{arm}, are constant with radius (giving logarithmic spirals) and drawn from a normal distribution centred on ϕ_{gal}, with some spread σ_{gal} common to all galaxies. We truncate this normal distribution between the physical limits of 0° (a ring) and 90° (a "spoke"), giving

$$\phi_{\mathrm{arm}} \sim \mathrm{TruncatedNormal}(\phi_{\mathrm{gal}}, \sigma_{\mathrm{gal}}, \min = 0, \max = 90). \qquad (3)$$

The choice to assume all galaxies show the same inter-arm variation in pitch angle (represented by a common value of σ_{gal} across all galaxies) was motivated by our small sample size and the low number of arms measured per galaxy.

We assume that the observed points in a *Galaxy Builder* spiral arm, once deprojected, follow a logarithmic spiral with gaussian radial error σ_r,

$$\widetilde{r_{\mathrm{arm}}} = \exp\left(\overrightarrow{\theta_{\mathrm{arm}}} \tan \phi_{\mathrm{arm}} + c_{\mathrm{arm}} \right). \qquad (4)$$

Where $\widetilde{r_{\mathrm{arm}}}$ is the model's predictions for the radii of the deprojected points in a *Galaxy Builder* arm ($\overrightarrow{r_{\mathrm{arm}}}$), and $\overrightarrow{\theta_{\mathrm{arm}}}$ is the polar angles of the points.

We choose hyperpriors over ϕ_{gal}, σ_{gal}, c_{arm} and σ_{r} of

$$\phi_{\mathrm{gal}} \sim \mathrm{Uniform}(\min = 0, \max = 90), \qquad (5)$$

$$\sigma_{\mathrm{gal}} \sim \mathrm{InverseGamma}(\alpha = 2, \ \beta = 20), \qquad (6)$$

$$c_{\mathrm{arm}} \sim \mathrm{Cauchy}(\alpha = 0, \ \beta = 10), \qquad (7)$$

$$\sigma_r \sim \mathrm{InverseGamma}(\alpha = 2, \beta = 0.5). \qquad (8)$$

The inverse gamma distribution is used to aid the convergence of the Hamiltonian Monte Carlo (HMC) algorithm used (discussed later). The Cauchy distribution is equivalent to the Student's t-distribution with one degree of freedom, and was chosen due to its fatter tails than the normal distribution. Our likelihood function for N arms, each with n_{arm} points, is

$$\mathcal{L} = \prod_{\mathrm{arm}=1}^{N} \left(2\pi\sigma_r^2 \right)^{-n_{\mathrm{arm}}/2} \exp\left(\frac{||\overrightarrow{r_{\mathrm{arm}}} - \widetilde{r_{\mathrm{arm}}}||^2}{2\sigma_r^2} \right). \qquad (9)$$

We assume that the radial error is Gaussian for simplicity of analysis, however, Shapiro-Wilk tests on the residuals of the logarithmic spirals fit in Lingard et al. (2020) suggest that this is not a good assumption, and a more robust likelihood (such as the Student's t-distribution) would possibly more appropriate.

To perform inference, we make use of the No-U-Turn-Sampler (NUTS, Hoffman & Gelman 2011), implemented in PYMC3[1], an open-source probabilistic programming framework written in Python (Salvatier et al. 2016). To aid the convergence of MC chains, we scale the radii of deprojected points to have unit variance.

3 RESULTS

3.1 Constraints on Galaxy Pitch angle

Our hierarchical model identifies the pitch angle of individual arms (ϕ_{arm}) with less than 1.6° of uncertainty for 95% of arms, assuming no error on disc inclination and position angle. The pitch angle of a galaxy as a whole (ϕ_{gal}), however, is not well constrained. This is primarily a result of only having pitch angles measurements for a small number of arms per galaxy, and reflects the difficulty in providing a single value for the pitch angle of a galaxy containing individual arms with very different pitch angles. For galaxies with two arms identified in *Galaxy Builder*, we have a mean uncertainty of ($\sigma_{\phi_{\mathrm{gal}}}$) of 7.9°, which decreases to 6.8° and 6.0° for galaxies with three and four arms respectively. This is roughly consistent with the standard error on the mean for a galaxy with N arms,

$$\sigma_{\phi_{\mathrm{gal}}} = \frac{\sigma_{\mathrm{gal}}}{\sqrt{N}}, \qquad (10)$$

where σ_{gal} is our measure of inter-arm variability of pitch angle and has a posterior distribution of 11.0° ± 0.9°. This variability is similar to that found by Kennicutt (1981) and Davis & Hayes (2014) and emphasises the need for fitting algorithms to not assume all arms have the same pitch angle. The spread of arm pitch angle from the mean galaxy pitch angle can be seen in Figure 2, with points colour-coded by the number of arms measured for a galaxy. We see a slight drop in $E[\phi_{\mathrm{gal}}]$ compared to $E[\phi_{\mathrm{arm}}]$ at small galaxy pitch angles, due to the truncation of ϕ_{gal} at 0°.

3.2 Dependence of pitch angle on Galaxy Morphology

In order to test the possible progenitor distribution of our estimated arm pitch angles, we repeatedly perform an Anderson-Darling test (Stephens 1974, implemented in SCIPY, Jones et al. 2001) over each draw present in the MC trace, resulting in a distribution of Anderson-Darling statistics. We will refer to this test as the *marginalized Anderson-Darling test*. We also make use of the two-sample Anderson-Darling (Scholz & Stephens 1987) test in a similar manner.

3.2.1 *Pitch angle vs. Bulge size*

Morphological classification commonly links bulge size to spiral tightness, and such a link is implied by the Hubble Sequence (Sandage 2005, Gadotti 2009, Buta 2013). Some studies have indeed reported a link between measured spiral galaxy pitch angle and bulge size (i.e. Hart et al. 2017, Davis
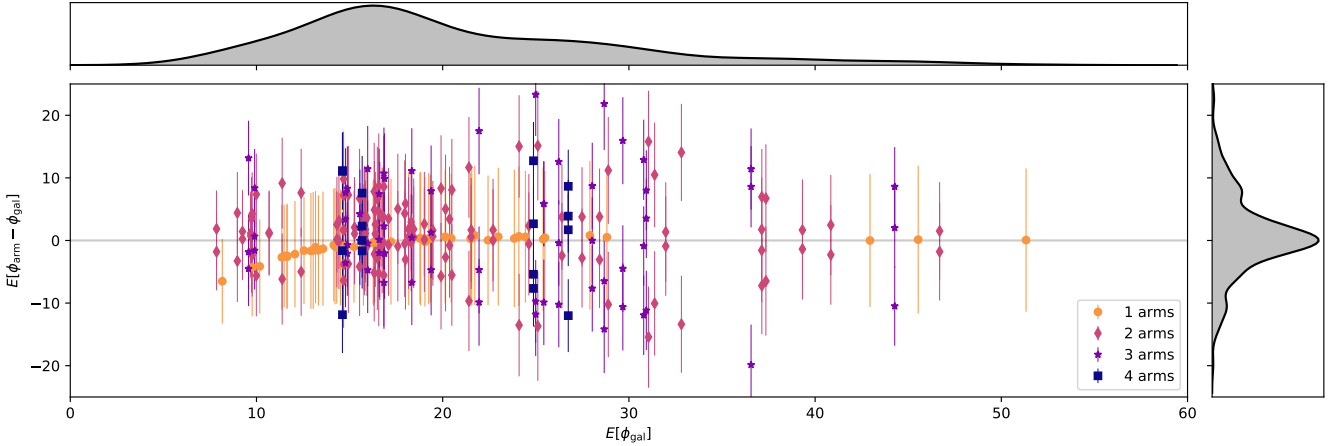
---

[1] `https://docs.pymc.io/`

Figure 2. Scatter plot showing how arm pitch angle compares to galaxy pitch angle for galaxies with different pitch angles and number of arms. The top panel shows a Gaussian KDE for $E[\phi_{gal}]$, and the right panel shows a Gaussian KDE for $E[\phi_{arm} - \phi_{gal}]$. The galaxy pitch angle is consistent with the mean of its arms, with large scatter and a slight bias against values near the lower bound of 0.

et al. 2019), while others have not found any significant correlation (Masters et al. 2019). We investigate this relationship here using a measure of bulge prominence from Galaxy Zoo 2, as Equation 3 in Masters et al. (2019):

$$B_{avg} = 0.2 \times p_{just\ noticeable} + 0.8 \times p_{obvious} + 1.0 \times p_{dominant}, \quad (11)$$

where $p_{just\ noticeable}$, $p_{obvious}$ and $p_{dominant}$ are the fractions of classifications indicating the galaxy's bulge was "just noticeable", "obvious" or "dominant" respectively.

We see no correlation between galaxy pitch angle derived from the hierarchical model and B_{avg}. The Pearson correlation coefficient between the expectation value of galaxy pitch angle ($E[\phi_{gal}]$) and B_{avg} is 0.00.

We separate our sample into galaxies with weaker bulges ($B_{avg} < 0.28$, 83 galaxies) and those with stronger bulges ($B_{avg} \geq 0.28$, 54 galaxies), in order to test whether their pitch angles could be drawn from significantly different distributions. A marginalized two-sample Anderson-Darling test comparing the distributions of ϕ_{gal} for the samples does not find evidence that galaxy pitch angles were drawn from different distributions: we reject the null hypothesis at the 1% level for only 1% of the samples. Similarly comparing arm pitch angles for galaxies in the different samples results in not rejecting the null hypothesis at the 1% level for any of the samples. The distributions of the Anderson-Darling test statistic for ϕ_{gal} and ϕ_{arm} are shown in the upper panel of Figure 3 in blue and orange respectively.

One limitation of this result is that our sample does not contain many galaxies with dominant bulges: B_{avg} only varied from 0.09 to 0.75 (the allowed maximum being 1.0), with only four galaxies having $B_{avg} > 0.5$. The split point of 0.28 was also chosen to produce evenly sized comparison samples rather than from some physical motivation. However, the lack of any form of correlation implies that there is no evidence in our data for the link between bulge size and pitch angle predicted by the Hubble sequence and observed in other studies.

3.2.2 Pitch angle vs. Bar Strength

One of the predictions of Manifold theory is that pitch angle increases with bar strength (Athanassoula et al. 2009b). In order to investigate this relationship in our data, we make use of Galaxy Zoo 2's bar fraction (p_{bar}), which has been demonstrated to be a good measure of bar length (Willett et al. 2013) and bar strength (Skibba et al. 2012, Masters et al. 2012) and therefore a good measure of the torque applied on the disc gas.

We do not observe a correlation between p_{bar} and $E[\phi_{gal}]$ (Pearson correlation coefficient of -0.05). Following Masters et al. (2012) and Skibba et al. (2012), we separate the sample into galaxies without a bar ($p_{bar} < 0.2$), with a weak bar ($0.2 \leq p_{bar} \leq 0.5$) and with a strong bar ($p_{bar} > 0.5$). Performing marginalized three-sample Anderson-Darling tests does not find that pitch angles (ϕ_{gal} or ϕ_{arm}) of galaxies with different bar strengths were drawn from different distributions; we do not reject the null hypothesis at the 1% level for any samples for the test of ϕ_{gal}, and at the 10% level for the test of ϕ_{arm}. The distributions of Anderson-Darling test statistic is shown in the lower panel of Figure 3.

We do not correct for variation in bulge size in this work, however, predictions from Manifold theory should not be affected as bulges do not provide a strong non-axisymmetric forcing. The fact that we do not find any link between bar strength and pitch angle suggests that the primary mechanism driving the evolution of the spirals in our sample is not Manifold theory.

3.3 Spiral Winding

For transient and recurrent spiral arms driven by self-gravity, Pringle & Dobbs (2019) suggest that spiral patterns form at some maximum pitch angle (ϕ_{max}), continually wind up over time and finally dissipate at some minimum pitch angle (ϕ_{min}). They propose that, under a set of very simple assumptions, the evolution of pitch angle would be governed by
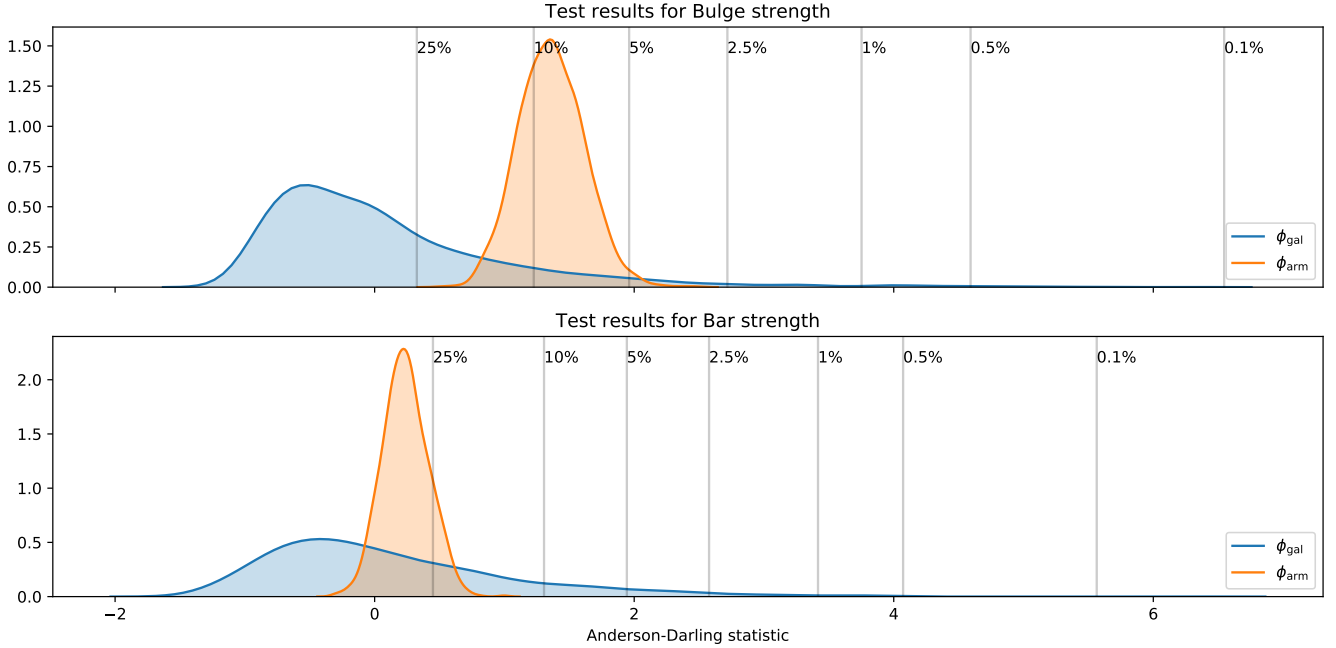
Figure 3. The results of marginalized two-sample Anderson-Darling tests examining whether pitch angles (ϕ_{gal} in blue and ϕ_{gal} in orange) for galaxies with $B_{\text{avg}} < 0.28$ and $B_{\text{avg}} \geq 0.28$ are drawn from the same distribution (top panel), and the results of marginalized three-sample Anderson-Darling tests for galaxies with no bar ($p_{\text{bar}} < 0.2$), a weak bar ($0.2 \leq p_{\text{bar}} \leq 0.5$) and a strong bar ($p_{\text{bar}} > 0.5$) (bottom panel). Confidence intervals are shown, with moving rightwards indicating more confidence in rejecting the null hypothesis that the compared values were drawn from the same parent distribution. We cannot reject the null hypotheis at the 1% level for any of the tests conducted.

$$\cot \phi = \left[R \frac{\mathrm{d}\Omega_p}{\mathrm{d}R} \right] (t - t_0) + \cot \phi_{\text{max}}, \qquad (12)$$

where Ω_p is the radially dependant pattern speed of the spiral arm and t_0 is the initial time at which it formed.

In QSDW theory, the pattern speed Ω_p is a constant in R, as spiral arms obey rigid-body rotation. If Ω_p instead varies with radius we would expect $\cot \phi$ to be uniformly distributed between $\cot \phi_{\text{max}}$ and $\cot \phi_{\text{min}}$.

In order to test this theory, Pringle & Dobbs (2019) used a Kolmogorov-Smirnov test to examine whether a sample of observed galaxy pitch angles was likely to have been drawn from a distribution uniform in its cotangent. Pitch angles were measured using discrete Fourier transformations in one- and two-dimensions, and as such do not account for inter-arm variations. They chose limits of $\cot \phi \in [1.00, 4.75]$ (roughly $11.9° < \phi < 45.0°$), motivated by examination of their data.

We aim to replicate their work here, using our sample and methods. We will make use of the marginalized Anderson-Darling test described above, and examine winding on a per-arm basis, as well as a per-galaxy basis. Observation of the distribution of arm pitch angles in our sample suggests limits of $15° < \phi < 50.0°$.

3.3.1 Galaxy Pitch angle

Testing the uniformity of $\cot \phi_{\text{gal}}$ between $15°$ and $50°$ using a marginalized Anderson-Darling test results in rejecting the

null hypothesis at the 1% level for just 5% of samples, with a large spread in observed test values. The full distribution of Anderson-Darling statistics can be seen in the upper panel of Figure 5. The large spread in results is caused by the large uncertainties in ϕ_{gal}.

This result suggests that we cannot rule out a cot-uniform source distribution for galaxy pitch angle, but the large uncertainty in ϕ_{gal} makes it difficult to make any conclusive statements. This result is also highly sensitive to the lower limit of ϕ: decreasing it to $10°$ results in us rejecting the cot-uniform model at greater than the 0.1% level for 96% of the posterior samples. As we have no information available on the biases present in *Galaxy Builder* spiral arm classification, we choose to keep the less strict limit of $15°$.

3.3.2 Arm Pitch angle

The inconclusive result for ϕ_{gal} is perhaps unsurprising: were we to assume that spiral arms are transient and recurrent instabilities, there is little reason for all of the arms to be at precisely the same evolutionary stage at the same time. This is supported by the large observed spread in inter-arm pitch angles.

If we assume instead that spirals form and wind independently in a galaxy, and that their evolution over time can be described by Equation 12, the distribution of the cotangent of pitch angles of individual arms should be uniform between our limits, rather than that of the galaxy's pitch angle as a whole.

Using the marginalized Anderson-Darling test we can-

not reject the null hypothesis at even the 5% level for any of the possible realizations of arm pitch angle. The resulting distribution of Anderson-Darling statistics is shown in in the lower panel of Figure 5. This result is highly consistent with the model for spiral winding proposed by Pringle & Dobbs (2019) and can be seen as evidence that spirals are formed through local disc perturbations, and are primarily governed by local forces.

4   SUMMARY

This paper presents a new Bayesian approach to estimate galaxy pitch angle, making use of citizen science results to measure spiral arms through photometric modelling. We introduce an adaptation of the Anderson-Darling test, which we name the *marginalized Anderson-Darling test*, to incorporate full Bayesian posterior probabilities and utilize this test to investigate theories governing spiral formation and evolution.

The hierarchical Bayesian approach implemented in this paper allows a more thorough examination of pitch angle than length-weighted pitch angle calculation; obtaining posterior distributions of measured parameters. It better accounts for the large variations observed in inter-arm pitch angle than Fourier analysis, which assumes all arms in a given mode have the same pitch angle. In this work, we find that the mean inter-arm difference in pitch angle is $11.0° \pm 0.9°$.

There is no evidence in our data for the link between bulge size and pitch angle predicted by the Hubble sequence and observed in other studies.

We do not find any link between bar strength and pitch angle suggests that the primary mechanism driving the evolution of the spirals in our sample is not Manifold theory.

Our results are consistent with spiral winding of the form described by Pringle & Dobbs (2019), in which spiral arms are transient and recurrent, evolve through mechanisms such as swing-amplification (Goldreich & Lynden-Bell 1965) and which wind up over time. However, the assumptions of this model of spiral winding are highly simplistic, and it leaves many unanswered questions: what determines the limits on ϕ? Is the spiral arm equally apparent at all pitch angles, or is a selection effect present? This result is also not evidenced against QSDW, as it is possible that our distribution of pitch angles is dictated by other factors such as disk shear.

In this work, we assume that spiral arms are equally likely to be identified and recovered at all pitch angles. This is not an unfair assumption given the amount of human effort that went into obtaining spiral arm measurements (more so than any other pitch angle measurement method, with each galaxy receiving 30 human classifications). The galaxy sample used is not guaranteed to be representative of the general spiral population, but is comparable in size to those used in other similar studies (Savchenko & Reshetnikov 2013, Yu & Ho 2019, Pringle & Dobbs 2019).

The methodology proposed here is a robust solution to the problems facing investigation of spiral morphology, namely that of reliably identifying spiral arms, and properly accounting for the spread in pitch angles of arms within a galaxy. As with most analyses, the most impactful improve-

ment it would be possible to make here would be to increase the cleanliness and volume of data analysed. A larger sample would make possible further comparisons, such as splitting galaxies into spiral type (grand design / many-armed / flocculent) and examining the differences between populations.

The processes governing the formation and evolution of spiral arms are immensely complicated, but the prevalence of spiral galaxies in the Universe, and the spiral nature of our own Milky Way, makes investigating their dynamics of fundamental importance to the scientific aims of understanding, predicting and explaining the nature of the cosmos.

References

Al-Baidhany I. A., Chiad S. S., Jabbar W. A., Hussein R. A., Hussain F. F. K., Habubi N. F., 2019, in Materials Science and Engineering Conference Series. p. 012118, doi:10.1088/1757-899X/571/1/012118

Athanassoula E., Romero-Gómez M., Masdemont J. J., 2009a, MNRAS, 394, 67

Athanassoula E., Romero-Gómez M., Bosma A., Masdemont J. J., 2009b, MNRAS, 400, 1706

Baba J., Saitoh T. R., Wada K., 2013, ApJ, 763, 46

Blanton M. R., Kazin E., Muna D., Weaver B. A., Price-Whelan A., 2011, AJ, 142, 31

Buta R., 1989, Galaxy Morphology. p. 151

Buta R. J., 2013, Galaxy Morphology. p. 155

Buta R. J., et al., 2015, VizieR Online Data Catalog, p. J/ApJS/217/32

Cedrés B., Cepa J., Bongiovanni Á., Castañeda H., Sánchez-Portal M., Tomita A., 2013, A&A, 560, A59

Davis D. R., Hayes W. B., 2014, ApJ, 790, 87

Davis B. L., Berrier J. C., Shields D. W., Kennefick J., Kennefick D., Seigar M. S., Lacy C. H. S., Puerari I., 2012, ApJS, 199, 33
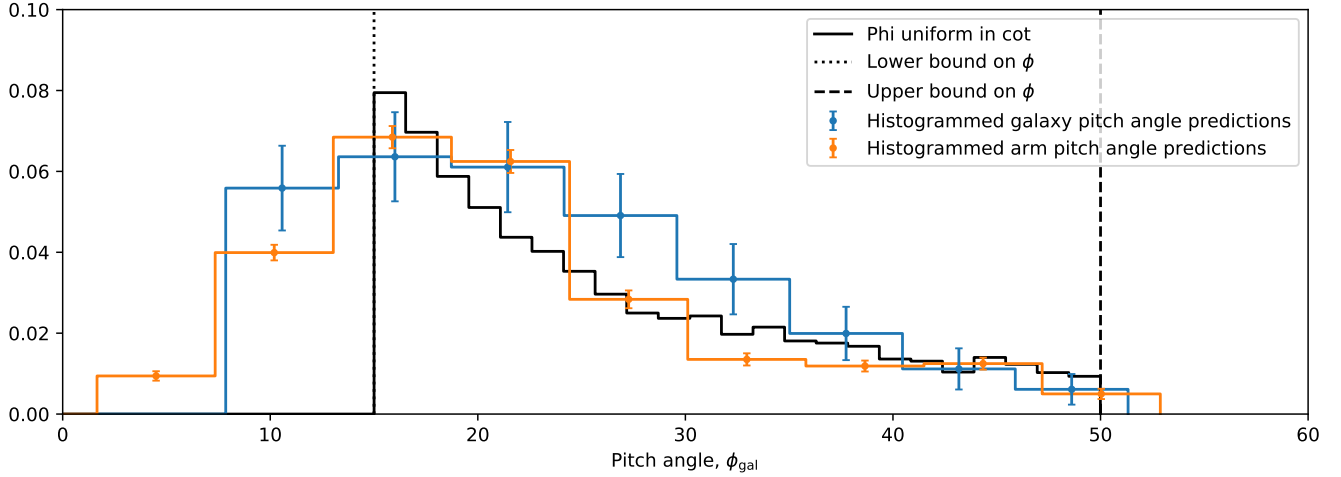
Figure 4. The distributions of pitch angles relative to one uniform in $\cot\phi$. Histograms have been normalised by the area between the limits such that they are comparable. The histogram was recalculated with identical bins for each posterior sample of ϕ_{gal} and ϕ_{arm}, we plot the mean value of each bin, with the sample standard deviation shown as errorbars. It is evident that the distributions are very similar between the chosen limits.
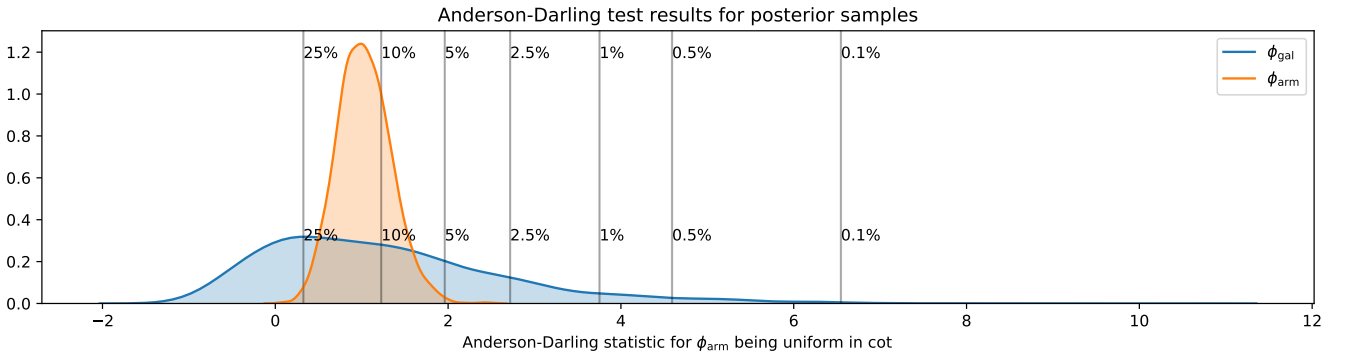

Figure 5. The results of a marginalized Anderson-Darling test for uniformity in $\cot$ for ϕ_{gal} (blue) and ϕ_{arm} (orange), with values corresponding to various confidence intervals shown. Moving rightwards on the x-axis implies greater confidence in rejecting the null hypothesis that the sample was drawn from a distribution uniform in $\cot$ between $15° < \phi < 50.0°$. In this instance, we would not be able to reject the null hypothesis at the 1% level for either ϕ_{gal} or ϕ_{arm}.

Davis B. L., Graham A. W., Seigar M. S., 2017, MNRAS, 471, 2187

Davis B. L., Graham A. W., Cameron E., 2019, ApJ, 873, 85

Díaz-García S., Salo H., Knapen J. H., Herrera-Endoqui M., 2019, arXiv e-prints, p. arXiv:1908.04246

Dobbs C. L., 2014, in Feltzing S., Zhao G., Walton N. A., Whitelock P., eds, IAU Symposium Vol. 298, Setting the scene for Gaia and LAMOST. pp 221–227 (`arXiv:1307.7133`), doi:10.1017/S1743921313006406

Dobbs C., Baba J., 2014, Publ. Astron. Soc. Australia, 31, e035

Elmegreen B. G., 2011, in Charbonnel C., Montmerle T., eds, EAS Publications Series Vol. 51, EAS Publications Series. pp 19–30 (`arXiv:1101.3109`), doi:10.1051/eas/1151002

Elmegreen D. M., et al., 2011, ApJ, 737, 32

Gadotti D. A., 2009, MNRAS, 393, 1531

Gao H., Ho L. C., 2017, ApJ, 845, 114

Goldreich P., Lynden-Bell D., 1965, MNRAS, 130, 125

Grand R. J. J., Kawata D., Cropper M., 2012, MNRAS, 426, 167

Hart R. E., et al., 2017, MNRAS, 472, 2263

Herrera-Endoqui M., Díaz-García S., Laurikainen E., Salo H., 2015, A&A, 582, A86

Hewitt I. B., Treuthardt P., 2020, MNRAS, 493, 3854

Hoffman M. D., Gelman A., 2011, arXiv e-prints, p. arXiv:1111.4246

Hubble E. P., 1926, ApJ, 64, 321

Jones E., Oliphant T., Peterson P., et al., 2001, SciPy: Open source scientific tools for Python, `http://www.scipy.org/`

Julian W. H., Toomre A., 1966, ApJ, 146, 810

Kennicutt R. C. J., 1981, AJ, 86, 1847

Kormendy J., Kennicutt Robert C. J., 2004, ARA&A, 42, 603

Lin C. C., Shu F. H., 1964, ApJ, 140, 646

Lingard T. K., et al., 2020, arXiv e-prints, p. arXiv:2006.10450

Lintott C. J., et al., 2008, MNRAS, 389, 1179

Mark J. W. K., 1976, ApJ, 205, 363

Masters K. L., et al., 2012, MNRAS, 424, 2180

Masters K. L., et al., 2019, MNRAS, 487, 1808

Mutlu-Pakdil B., Seigar M. S., Hewitt I. B., Treuthardt P., Berrier J. C., Koval L. E., 2018, MNRAS, 474, 2594

Peng C. Y., Ho L. C., Impey C. D., Rix H.-W., 2010, AJ, 139, 2097

Pringle J. E., Dobbs C. L., 2019, arXiv e-prints, p. arXiv:1909.10291

Ringermacher H. I., Mead L. R., 2009, MNRAS, 397, 164

Rodriguez-Fernandez N. J., Combes F., 2008, A&A, 489, 115

Romero-Gómez M., Masdemont J. J., Athanassoula E., García-Gómez C., 2006, A&A, 453, 39

Salvatier J., Wiecki T. V., Fonnesbeck C., 2016, PeerJ Computer Science, 55

Sandage A., 1961, The Hubble Atlas of Galaxies

Sandage A., 2005, ARA&A, 43, 581

Sanders R. H., Huntley J. M., 1976, ApJ, 209, 53

Savchenko S. S., Reshetnikov V. P., 2013, MNRAS, 436, 1074

Scholz F. W., Stephens M. A., 1987, Journal of the American Statistical Association, 82, 918

Seigar M. S., Block D. L., Puerari I., Chorney N. E., James P. A., 2005, MNRAS, 359, 1065

Seigar M. S., Kennefick D., Kennefick J., Lacy C. H. S., 2008, ApJ, 678, L93

Skibba R. A., et al., 2012, MNRAS, 423, 1485

Stephens M. A., 1974, Journal of the American Statistical Association, 69, 730

Willett K. W., et al., 2013

Yoshizawa M., Wakamatsu K., 1975, A&A, 44, 363

Yu S.-Y., Ho L. C., 2019, ApJ, 871, 194

de Vaucouleurs G., de Vaucouleurs A., Corwin Herold G. J., Buta R. J., Paturel G., Fouque P., 1991, Third Reference Catalogue of Bright Galaxies

This paper has been typeset from a TeX/LaTeX file prepared by the author.